Journal of Life Science 2008 Vol. 18. No. 11. 1513~1520 ©JLS / ISSN 1225-9918

4-Hydroxynonenal Induces Endothelial Apoptosis through Mitochondrial Depolarization

Dae Yeon Kang[1,3†], Ji Young Lee[1,2†], Min-Sun Kim[1], Chul Hong Kim[1,3], Hyung Keun Kim[1,3], Sun Mi Lee[1,3], Young Mi Kwon[1,3], Jaewon Lee[1], Hyung Suk Baik[3], Byung Pal Yu[4] and Hae Young Chung[1]*

[1]*College of Pharmacy, Pusan National University, Busan 609-735, Korea*
[2]*MRC for Ischemic Tissue Regeneration, College of Medicine, Pusan National University, Busan 602-739, Korea*
[3]*Genetic Engineering Research Institute, Pusan National University, Busan, 609-735, Korea*
[4]*Department of Physiology, The University of Texas Health Science Center at San Antonio, TX, 78229-3900, USA*

Received September 17, 2008 / Accepted October 27, 2008

The 4-Hydroxynonenal (HNE) affects vascular dysfunctions probably through the interruption of the cellular redox balance. To better understand vascular abnormalities resulting from the accumulation of HNE, we delineated mechanism by which mitochondrial apoptosis occurs in the YPEN-1 endothelial cells. HNE treatment led to the loss of mitochondrial membrane potential ($\delta\Psi_m$), resulting in the release of cytochrome *c*. Data showed decreased Bcl-2 and increased Bax protein levels in HNE-treated cells. NAC, a reactive oxygen species (ROS) scavenger, and penicillamine, the peroxynitrite scavenger, blocked HNE-mediated ROS generation, thereby thwarting the cytochrome *c* release and apoptosis. The treatment of the cells with zVAD-fmk, a broad range caspase inhibitor did not suppress HNE-induced apoptosis, suggesting that the apoptosis might be the possibility of caspase-independent process. Our findings delineate the underlying mechanism of the HNE induced endothelial apoptosis by triggering depolarization of mitochondria membrane potential that can lead to the deterioration of vasculature homeostasis and subsequent vascular dysfunction with aging.

Key words : 4-Hydroxynonenal, apoptosis, mitochondrial membrane potential, caspase-3, cytochrome C release

Introduction

Endothelial cell aging, with its accompanying vascular dysfunctions, is regarded as a fundamental defect inducing tissue and whole-body aging [40]. Because vascular endothelial cells line the blood vessel wall and serve as a primary barrier, they are under constant attack from oxidative stress caused by various oxidized lipids and proteins in the plasma [21]. Evidence shows that increased accumulation of senescent cells and apoptosis are found in vascular endothelium during aging [23]. Thus, the endothelial cell apoptotic process could play a significant role not only in the normal aging, but also in the progression of age-related vascular diseases.

The activity of reactive aldehydes, such as 4-hydroxynonenal (HNE), 4-hydroxyhexenal (HHE), and malondialdehyde (MDA), exacerbate under enhanced lipid peroxidation [8,12]. These reactive aldehydes are known to cause redox disturbances and various degenerative processes, including the vascular dysfunction associated with aging [12,20,37]. It seems logical that HNE and HHE are the subjects of recent intensified studies investigating their roles in the modulation of cell signaling pathways and the induction of apoptosis [2,15,36]. HNE as a potent cytotoxic agent is a byproduct of n-6 fatty acid peroxidation [12,35], which can accumulate up to concentrations of 10 μM to 5 mM both *in vivo* and *in vitro* [8,33]. HNE generated by oxidative stress is thought to lead cells to apoptosis [20,23], pulmonary edema [10], and cardiovascular disorders such as atherosclerosis [34]; however, the involvement of HNE in vascular endothelial dysfunction is unclear and not well studied.

Accumulating evidence established mitochondria as a centerpiece of the apoptotic process. For instance, Pollack and Leeuwenburgh [28] reported that cell loss is directly mediated through mitochondrial dysfunction caused by chronic exposure to oxidants and increased activation of mitochondrial permeability transition (MPT).

Kristal et al. [26] found that HNE and HHE are extremely

***Corresponding author**
Tel : +82-51-510-2814, Fax : +82-51-518-2821
E-mail : hyjung@pusan.ac.kr
†Both authors contributed equally to this work

effective in inducing MPT, which leads to disruptions of calcium homeostasis and mitochondrial transcription. Recently, the mitochondrial dysfunction was turned out to be caused by mitochondrial depolarization in human aortic endothelial cell apoptosis [28,29]. Nevertheless, HNE's ability to induce vascular endothelial cell dysfunction through the regulation of mitochondrial apoptosis is not yet well described. Accordingly, it is important to define the role of HNE in vascular endothelial apoptosis in relation to mitochondrial dysfunction.

Apoptotic process can occur by important mitochondrial changes. These changes include alterations in the mitochondrial membrane potential ($\delta\Psi_m$), mitochondrial transport, and the release of proteins like cytochrome *c* into the cytoplasm [3,27]. These events could result in ATP loss, membrane alterations, DNA condensation, and the activation of pro-apoptotic caspases [9]. Released cytochrome *c* activates the caspase cascade, which leads to the terminal steps of caspase-dependent apoptosis [16].

Based on present available data for the impact of oxidative stress on the mitochondrial apoptosis pathway, we propose that HNE induces apoptosis in vascular endothelial cells via a mechanism that involves the mobilization of the mitochondrial cytochrome *c* under the control of the Bcl-2 family proteins, Bcl-2 and Bax. To investigate the involvement of pertinent factors in HNE-induced apoptosis, the anti-oxidants, N-acetyl cysteine (NAC), a peroxynitrite ($ONOO^-$) scavenger, and zVAD-fmk (a potent caspase inhibitor) were utilized in the study. The data obtained from the present study provide further molecular insights into the role of lipid peroxidation in the apoptosis and $\delta\Psi_m$.

Materials and Methods

Cell line and culture condition

YPEN-1 cells, rat prostate endothelial cells, were obtained from ATCC (American Type Culture Collection, USA). The cells were grown in DMEM (Dulbecco's Modified Eagle Medium Media, Nissui, Tokyo, Japan) containing 2 mM L-glutamine, 100 mg/ml streptomycin, 2.5 mg/l amphotericin B and 5% heat-inactivated fetal bovine serum (FBS). Cells were maintained at 37°C in a humidified atmosphere containing 5% CO_2/95% air. Cells were discarded after 3 months, at which time new cells were obtained from frozen stock. Cells at the exponential phase were used for all experiments, and cell viability (>90%) was assessed by trypan blue exclusion.

Treatments of cells with HNE, antioxidants and caspase-inhibitor

Commercial HNE, 4-hydroxynonenal (purity >98%; Cat. No. 32060), was obtained from Cayman Chemical Inc. Working solutions of HNE (<0.1% ethanol) were made in PBS immediately before use. For all experiments, cells were plated in 100 mm culture dishes and cultures at 70% confluences were used for the chemical exposures. After 24 hr attachment period, media were replaced with serum free media, and cells were treated with 10 μM HNE after pre-incubation for 30 min with NAC (300 μM), penicillamine (300 μM) and zVAD-fmk (50 μM). After 1 to 6 hr, cells were harvested and washed with ice-cold PBS, and cells lysates were used for Western blot analysis.

Analysis of the intracellular reactive oxygen species (ROS) levels by confocal laser microscopy

Intracellular reactive oxygen species were monitored by dichlorofluorescein (DCF) fluorescence and visualized by confocal laser microscopy [6]. The amount of $ONOO^-$ generated was estimated by assaying formation of fluorescent rhodamine-123 from the oxidation of non-fluorescent dihydrorhodamine-1,2,3 (DHR 123) according to the modified method of McBride et al. [5]. Briefly, cells grown to sub-confluence on glass cover slips were incubated with HNE. Following stimulation for 2 hr, cells were washed with PBS and then incubated with 10 μM 2′,7′-dichlorofluorescin diacetate (DCF-DA, Molecular Probes, USA) or DHR 123 for an additional 20 min. The cells were washed with PBS and mounted in the microscope stage. Fluorescence images were recorded using a Zeiss LSM 510 laser scanning confocal microscope with excitation at 488 nm and long-pass detection at 530 nm. A fluorometric assay was performed to determine the relative levels of ROS, such as superoxide radical, hydroxyl radical, and hydrogen peroxide [6]. This assay measures the oxidative conversion of stable, nonfluorescent DCF-DA to the highly fluorescent DCF in the presence of esterases and reactive species [30]. This probe has been used extensively for quantification of ROS and lipid hydroperoxides after careful examination for potential pitfalls in the assay conditions [1].

Measurement of ROS generation

The RS generation was quantified by measuring the

changes in the fluorescent intensity of DCF. Briefly, DCF-DA was added to cell lysates in a 96-well plate to achieve a final concentration of 25 μM. The plates were incubated at 37°C for 30 min in the presence of exogenously added esterase (0.3 U at a final concentration) to ascertain a steady-level of DCF. The level in fluorescence intensity was monitored using a microplate fluorescence reader (Bio-TEK Instruments, Inc., Winooski, VT, USA) at excitation 485 nm/emission 530 nm. ROS levels were expressed as fluorescence intensity per milligram of protein.

Protein analysis by Western blot

Western blotting was carried out as described previously [13]. Cells were harvested, washed twice with ice-cold PBS, and lysed in a TNN buffer (50 mM Tris-HCl, pH 8.0, 120 mM sodium chloride, 0.5% Nonidet P-40) that was supplemented with protease inhibitors (2 μg/ml aprotinin, 2 μg/ml leupeptin, and 100 μg/ml PMSF, and 5 μg/ml pepstatin, 1 mM DTT) and phosphates inhibitors (20 mM NaF and 2 mM Na_3VO_4) for 1 hr on ice, vortexing after every 10 min. Lysates were centrifuged at 12,000 rpm for 30 min to remove insoluble material. The protein concentration was determined by Lowry method (Sigma, USA) using bovine serum albumin (BSA) as a standard. Equal amounts of protein were separated on 10-15% SDS-PAGE. The gels were subsequently transferred onto a nitrocellulose membrane (Hybond C, Amersham Corp.). Monoclonal antibodies (Bcl-2 and caspase-3) and polyclonal antibodies (Bax and cytochrome c) were purchased from Santa Cruz Biotechnology Inc. (Santa Cruz, CA, USA). Monoclonal sheep anti-mouse IgG, or donkey anti-rabbit IgG horseradish peroxidase-conjugated secondary antibodies were used at 1:1,000 dilution. Proteins were detected by an enhanced chemiluminescence (ECL) reagent using a commercial kit (Amersham Life Science, Arlington HTs, IL, USA).

Measurements of mitochondrial membrane potential ($\delta\Psi m$)

The rhodamine 123 (Molecular Probes, USA) was used as a measure of $\delta\Psi_m$ according to methods described previously [18]. In brief, cells grown to sub-confluence on glass cover slips were incubated with HNE. Following stimulation for 3 hr, cells were incubated with 10 μM of the dye for an additional 30 min. Then, cells were washed with PBS. Cellular fluorescence was imaged using a Zeiss LSM 510 laser scanning confocal microscope with excitation at 488 nm.

Analysis of cytochrome c release

The release of mitochondrial cytochrome c was determined by Western blot [19]. Briefly, cells were washed twice with ice-cold PBS and resuspended in ice-cold lysing buffer (50 μl of HEPES, pH 7.5, containing 10 mM KCl, 1.5 mM $MgCl_2$, 5 mM EDTA, 1 mM DTT, 2 mM PMSF, 2 μg/ml aprotinin, 2 μg/ml leupeptin, 5 μg/ml pepstatin, 250 mM sucrose, and 150 μM digitonin). Then, cells were vortexed for 10 seconds at low speed and were centrifuged for 4 min at 3,000 rpm at 4°C. The supernatant was further centrifuged for 10 min at 12,000 rpm and then loaded on 15% SDS gel. After electrophoretic separation, the proteins were transferred to nitrocellulose membrane (Hybond C, Amersham Corp) and the blot was incubated with monoclonal anti-cytochrome *c* antibody (Santa Cruz Biotechnology Inc. Santa Cruz, CA, USA), followed by reaction with horseradish peroxidase-conjugated secondary antibody.

Statistics

ANOVA was conducted to analyze significant differences among all groups. Difference among the means of individual groups was assessed by the Fischer's Protected LSD post hoc test. Values of $p < 0.05$ were considered statistically significant.

Results and Discussion

Free radical-mediated lipid peroxidation and its reactive byproducts, like HNE are known to cause cellular structural perturbations and various redox-related degenerative processes, including vascular dysfunction [12,20,36]. To assess the HNE-induced oxidative stress in vascular endothelial cells, we analyzed ROS production using confocal microscopy. As shown in Fig. 1, ROS levels increased in HNE-treated (5 and 10 μM) YPEN-1 cells, compared to the untreated control cells. Further, treatment with 10 μM HNE increased the fluorescence intensity in ROS levels more than that of 5 μM HNE, indicating a does-dependent generation of ROS by HNE. Under normal and pathological conditions, endogenous concentrations of HNE may increase significantly and accumulate in cellular membranes as much as 5 mM in response to oxidative stress as reported [12,33]. Under these conditions, the concentration of 10 μM in our study could play significant role. Depolarization of mitochondrial membrane ($\delta\Psi_m$) is an early event of apoptosis [41]. We monitored changes in $\delta\Psi_m$ by loading mitochondria

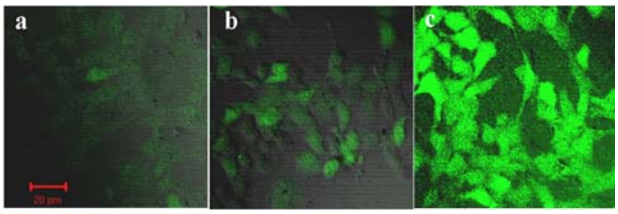

Fig. 1. Induction of ROS generation by HNE. Analysis of intracellular ROS generation induced by HNE using confocal laser microscopy. Cells were incubated in serum free media with the HNE (5 μM and 10 μM) for 3 hr, in which the concentration (5 μM and 10 μM) were used to avoid the HNE binding with albumin. DCF-DA method was used to determine the intracellular RS generation as described in Materials and Methods. Panels showed images of fluorescence and phase contrast. Panel a, control; Panel b, HNE (5 μM); Panel c, HNE (10 μM). The results are representative of three independent experiments.

with rhodamine 123 [39], a cationic fluorophore taken up by mitochondria because of the negatively charged matrix. The uptake of rhodamine 123 was visualized by a laser scan confocal microscopy. As shown in Fig. 2, the fluorescent intensities decreased as a result of the loss of $\delta\Psi_m$ (see the arrow) in the YPEN-1 cells treated with 10 μM HNE for 3 hr. These observations indicate that HNE induced loss of $\delta\Psi_m$, resulting in cytochrome *c* release. In this study, we obtained evidence of cytochrome *c* release and caspase-3, which most likely occurred following mitochondrial depolarization by the action of HNE. It was reported that HNE could lead to the release of cytochrome *c* from in mitochondria in RAW 264.7 cells [15]. The pre-apoptotic $\delta\Psi_m$ disruption, i.e., membrane depolarization, was expected to mediate a change in MPT, in which the opening of the mitochondrial megachannel appears to be critical to the apoptotic process [19]. The interrelationship of mitochondrial depolarization and MPT has been reported [32]. As the dissipation of $\delta\Psi_m$ was associated with the release of cytochrome c from mitochondria, Western blot analysis for cytochrome c and caspase-3 were carried out. The results show that the disruption of the mitochondrial membrane by HNE caused changes in the membrane potential followed by the release of cytochrome *c* into the cytoplasm (Fig. 3A) and cleavage of caspase-3 (Fig. 3B). Anti-apoptotic proteins, e.g., Bcl-2, are thought to exert an inhibitory action against the cytochrome *c* release, thereby protecting the cell from apoptosis [39]. The effectiveness of Bcl-2 against cytochrome *c* release is modulated by the counteraction of the pro-apoptotic protein, Bax. For instance, when Bax dominates Bcl-2,

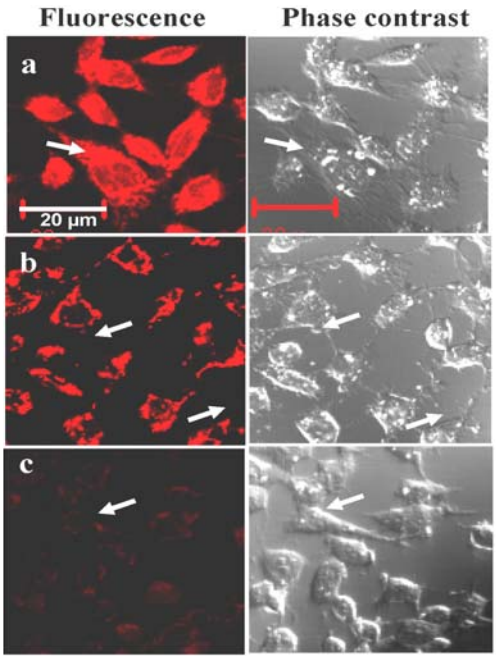

Fig. 2. Images of membrane potential ($\delta\Psi_m$) in mitochondria. Panels show images of fluorescence and phase contrast, respectively. Panel a, control; Panel b, HNE (5 μM); Panel C, (10 μM). Cellular fluorescence was imaged using a Zeiss LSM 510 laser scanning confocal microscope with excitation wavelength of 488 nm.

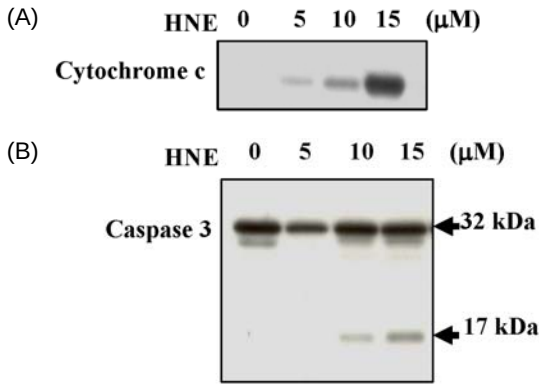

Fig. 3. Induction of cytochrome *c* release and caspase-3 activation by HNE. The cells were incubated in serum-free media with 10 μM HNE for 6 hr. (A) The release of cytochrome *c* into cytosol; (B) Activation of caspase-3. The cytosol fraction was separated as described under 'Material and Methods'. The levels cytochrome *c* and caspase-3 were analyzed by Western blot. The results are representative of three independent experiments.

cytochrome *c* is liberated from the mitochondrial membrane [25]. As shown in Fig. 4A, the Bcl-2 protein level was decreased by 10 μM HNE treatment, while the level of the Bax protein was increased (Fig. 4B), indicating that HNE caused

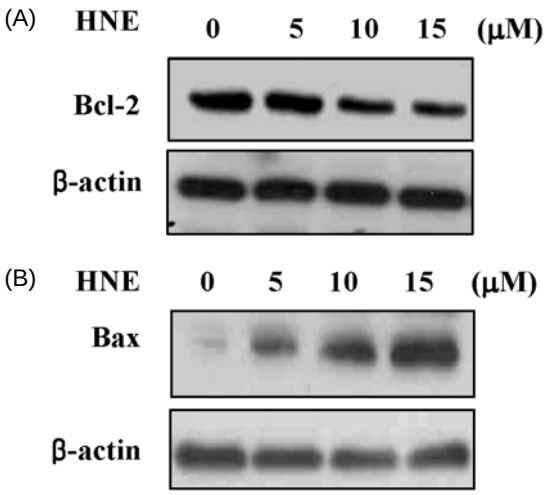

Fig. 4. Modulation of Bcl-2 and Bax by HNE. Down-regulation of Bcl-2 (A); up-regulation of Bax (B). The cells were incubated for 6 hr in serum-free media with or without HNE. The protein concentration equivalent to the whole cell was analyzed by Western blot analysis. The data presented are representative of at least 3 separate experiments.

endothelial apoptosis through the enhancement of apoptotic Bax and the suppression of anti-apoptotic Bcl-2. Mikhailov and coworkers [22] found that Bcl-2 protect cells from apoptosis by preventing Bax oligomerization in the outer mitochondrial membrane. Data on our findings regarding the HNE activation on Bcl-2 (Fig. 4) suggest HNE reduces transcription of Bcl-2. Lipid peroxidation causes a loss of mitochondrial $\delta\Psi_m$, thereby releasing cytochrome *c* into cytosol, leading to apoptotic cell death. Cheng et al. [7] reported that HNE mediates apoptosis through its effects on c-Jun N-terminal protein kinase (JNK) and caspase-3, and modulates oxidative stress-induced apoptosis by regulation of glutathione S-transferase (GST). Also it was reported that, in vascular smooth muscle cells, HNE promote apoptotic cell death through nuclear factor kappa B (NF-κB) activation [31]. Additional evidence showing HNE as a potent mediator of apoptosis through cytochrome *c* in RAW 264.7 cells was reported by Haynes et al. [15]. Although apoptosis induced by HNE via cytochrome *c* release and caspase-3 activation in human colorectal carcinoma and HL-60 cells have been reported by Anuradha et al. [2], they didn't performed the experiment with ROS inhibitors such as NAC or penicillamine. In our study, the utilization of inhibitors let us to define or identify the specific factors involved in HNE-induced apoptotic process. To verify the possible involvement of $ONOO^-$ generated in HNE-induced mitochondrial dysfunction leading to endothelial cell apoptosis, we measured intracellular $ONOO^-$ levels in NAC- or penicillamine-treated YPEN-1 cells. When fluorescent probe DHR 123 is oxidized by ROS such as $ONOO^-$, fluorescence intensity is accumulated in mitochondria [19]. As can be seen in Fig. 5, the level of $ONOO^-$ levels in HNE-exposed cells were increased, compared with untreated controls (see the arrow in panel b). The NAC (an RS scavenger) and penicillamine ($ONOO^-$ scavenger) suppressed generation of intracellular $ONOO^-$ induced by HNE (see the arrow in panel c and d). Also, NAC and penicillamine blocked the HNE-induced cytochrome *c* release (Fig. 5B). To further examine whether the HNE-induced apoptosis involves caspase activation, we tested the caspase activity in the presence of a

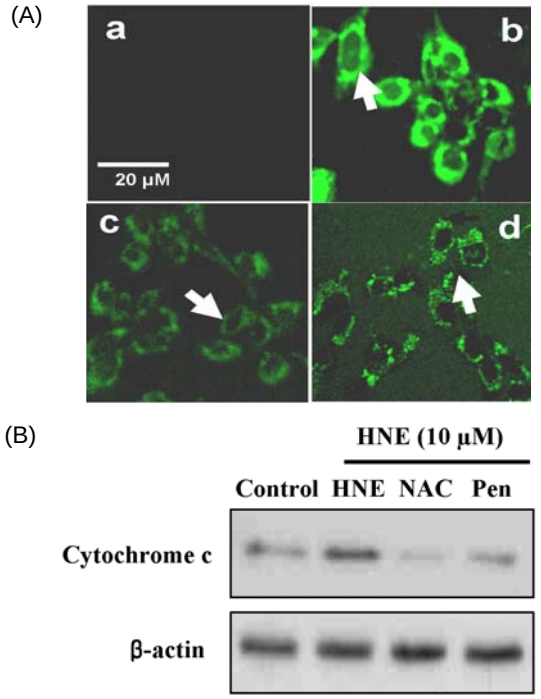

Fig. 5. Inhibitory effects of NAC and penicillamine on ROS-mediated cytochrome *c* release and caspase-3 activation by HNE. (A) Microscope analysis of intracellular $ONOO^-$ levels by confocal laser. The cells were incubated in serum-free media with 10 μM HNE for 2 hr after pre-treatment for 30 min with 300 μM NAC or 300 μM penicillamine. Panel a, control; Panel b, 10 μM HNE; Panel c, 10 μM HNE + 300 μM NAC; Panel d, 10 μM HNE + 300 μM penicillamine. Western blotting analysis of cytosolic cytochrome *c* (B) in whole cell protein. The cells were incubated in serum free media with the 10 μM HNE for 6 hr after pre-treatment for 30 min with 300 μM NAC or 300 μM penicillamine. The data presented are representative of at least 3 separate experiments.

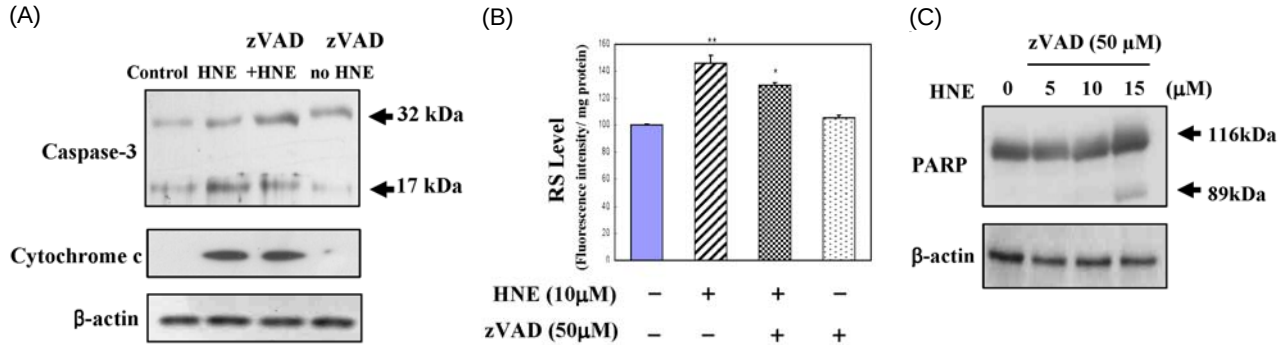

Fig. 6. Effects of HNE and zVAD-fmk on cytochrome *c* release and caspase-3, and ROS generation. The cells were incubated in serum free media with the 10 μM HNE for 6 hr after pre-treatment for 30 min with 50 μM zVAD. (A) The release of cytochrome c into cytosol and inhibition of caspase-3 by zVAD. (B) The effect of HNE and zVAD on ROS generation that was quantified by DCF changes in the cell lysates as described in the "Experimental procedures". * $P<0.05$, ** $P<0.01$ vs. untreated control. (C) The effect of HNE and zVAD on PARP cleavage. The data presented are representative of at least 3 separate experiments.

non-specific caspase inhibitor zVAD-fmk. As shown in the Fig 6A, preincubation with zVAD-fmk (50 μM) suppressed slightly the HNE induced caspase-3 cleavage, while did not prevent apoptosis and poly(ADP-ribose) polymerase (PARP) cleavage (Fig. 6C), indicating that the HNE-induced cytochrome *c* release may be nothing to do with caspase-dependent pathway. The proteolytic cleavage of PARP is a terminal event occurring in apoptosis that involves DNA fragmentation [4,38]. A recent paper by Kang et al. [17] reported the PARP cleavage leading apoptosis without caspase-3 activation. Our data on cytochrome *c* release (Fig. 6A) and ROS generation (Fig. 6B) concur with the occurrence of apoptosis without caspase-3 activation. Generally, the involvement of caspase mediated apoptosis has been accepted. However, our new data clearly indicate that some of apoptotic phenomena are carried out by caspase-independent pathway [24]. A recent review by Donovan and Cotter [11] highlighted the caspase-independent cell death as an important characteristic of programmed cell death. Based on our data from the effects of NAC and penicillamine, HNE-induced apoptosis is most likely mediated through HNE-initiated oxidative stress on mitochondrial depolarization to release pro-apoptotic factors from the mitochondrial intermembrane space, resulting in cell death.

In summary, our findings demonstrated that HNE triggered apoptosis through the release of cytochrome *c* without caspase activation. Thus, the induction of mitochondrial ROS generation by HNE may be the priciple causative for the endothelial apoptosis. This new information on the initiation of mitochondrial membrane depolarization by HNE, resulting in caspase-independent endothelial apoptosis offers better molecular mechanism for further exploration.

Acknowledgement

This research was supported by a Korea Research Foundation Grant (KRF-2003-005-C00031). We are thankful to the Aging Tissue Bank supplying aged tissue.

References

1. Ali, S. F., C. P. LeBel and S. C. Bondy. 1992. Reactive oxygen species formation as a biomarker of methylmercury and trimethyltin neurotoxicity. *Neurotoxicology* **13**, 637-648.
2. Anuradha, C. D., S. Kanno and S. Hirano. 2001. Oxidative damage to mitochondria is a preliminary step to caspase-3 activation in fluoride-induced apoptosis in HL-60 cells. *Free Radic. Biol. Med.* **31**, 367-373.
3. Arita, K., H. Kobuchi, T. Utsumi, Y. Takehara, J. Akiyama, A. A. Horton and K. Utsumi. 2001. Mechanism of apoptosis in HL-60 cells induced by n-3 and n-6 polyunsaturated fatty acids. *Biochem. Pharmacol.* **62**, 821-828.
4. Bursztajn, S., J. J. Feng, S. A. Berman and A. Nanda. 2000. Poly (ADP-ribose) polymerase induction is an early signal of apoptosis in human neuroblastoma. *Brain Res. Mol. Brain Res.* **76**, 363-376.
5. Cathcart, A. G., V. Borutaite and G. C. Brown. 1999. Superoxide dismutase and hydrogen peroxide cause rapid nitric oxide breakdown, peroxynitrite production and subsequent cell death. *Biochim. Biophys. Acta.* **1454**, 275-288.
6. Cathcart, R., E. Schwiers and B. N. Ames. 1983. Detection of picomole levels of hydroperoxides using a fluorescent dichlorofluorescein fluorescent assay. *Anal. Biochem.* **134**, 111-116.

7. Cheng, J. Z., S. S. Singhal, A. Sharma, M. Saini, Y. Yang, S. Awasthi, P. Zimniak and Y. C. Awasthi. 2001. Transfection of mGSTA4 in HL-60 cells protects against 4-hydroxynonenal-induced apoptosis by inhibiting JNK-mediated signaling. *Arch. Biochem. Biophys.* **392**, 197-207.
8. Chiarpotto, E., F. Biasi, A. Scavazza, S. Camandola, M. U. Dianzani and G. Poli. 1995. Metabolism of 4-hydroxy-2-nonenal and aging. *Bioche. Biophys. Res. Commun.* **207**, 477-484.
9. Colquhoun, A. and R. I. Schumacher. 2001. ɣ-Linolenic acid and eicosapentaenoic acid induce modifications in mitochondrial metabolism, reactive oxygen species generation, lipid peroxidation and apoptosis in Walker 256 rat carcinosarcoma cells. *Biochim. Biophys. Acta.* **1533**, 207-219.
10. Compton, C. N., A. P. Franko, M. T. Murray, L. N. Diebel and S. A. Dulchavsky. 1998. Signaling of apoptotic lung injury by lipid hydroperoxides. *J. Trauma.* **44**, 783-788.
11. Donovan, M. and T. Cotter. 2004. Control of mitochondrial integrity by Bcl-2 family members and caspase-independent cell death. *Biochim. Biophy. Acta.* **1644**, 133-147.
12. Esterbauer, H., R. J. Schaur and H. Zollner. 1991. Chemistry and biochemistry of 4-hydroxynenenal, malonaldehyde and related aldehydes. *Free Radic. Biol. Med.* **11**, 81-128.
13. Habib, A., C. Creminon, Y. Frobert, J. Grassi, P. Pradelles and J. Maclouf. Demonstration of an inducible cyclooxygenase in human endothelial cells using antibodies raised against the carboxyl-terminal region of the cyclooxygenase-2. *J. Biol. Chem.* **268**, 23448-23454.
14. Hamilton Jr., R. F., L. Li, W.L. Eschenbacher, L. Szweda and A. Holian. 1998. Potential involvement of 4-hydroxynonenal in the response of human lung cells to ozone. *Am. J. Physiol.* **274**, 8-16.
15. Haynes, R. L., B. Brune and A. J. Townsend. 2001. Apoptosis in RAW 264.7 cells exposed to 4-hydroxy-2-nonenal: dependence on cytochrome C release but not p53 accumulation. *Free Radic. Biol. Med.* **30**, 884-894.
16. Joza, N., S. A, Susin, E. Daugas, W. L. Stanford, S. K. Cho, C. Y. Li, T. Sasaki, A. J. Elia, H. Y. Cheng, L. Ravagnan, K. F. Ferri, N. Zamzami, A. Wakeham, R. Hakem, H. Yoshida, Y. Y. Kong, T. W. Mak, J. C. Zuniga-Pflucker, G. Kroemer and J. M. Penninger. 2001. Essential role of the mitochondrial apoptosis-inducing factor in programmed cell death. *Nature* **410**, 549-554.
17. Kang, Y. H., M. J. Yi, M. J. Kim, M. T. Park, S. Bae, C. M. Kang, C. K. Cho, I. C. Park, M. J. Park, C. H. Rhee, S. I. Hong, H. Y. Chung, Y. S. Lee and S. J. Lee. 2004. Caspase-independent cell death by arsenic trioxide in human cervical cancer cells: reactive oxygen species-mediated poly (ADP-ribose) polymerase-1 activation signals apoptosis-inducing factor release from mitochondria. *Cancer Res.* **64**, 8960-8967.
18. Kruman, I. I. and M. P. Mattson. 1999. Pivotal role of mitochondrial calcium uptake in neural cell apoptosis and necrosis. *J. Neurochem.* **72**, 529-540.
19. Kruman, P., M, Castedo, S. A, Susin, N, Zamzami, T. Hirsch, A. Macho, A. Haeffner, F. Hirsch, M. Geuskens and G. Kroemer. 1996. Mitochondrial permeability transition is a central coordinating event of apoptosis. *J. Exp. Med.* **184**, 1155-1160.
20. Lee, J. Y., J. H. Je, D. H. Kim, S. W. Chung, Y. Zou, N. D. Kim, M. A. Yoo, H. S. Baik, B. P. Yu and H. Y. Chung. 2004. Induction of endothelial apoptosis by 4-hydroxyhexenal. *Eur. J. Biochem.* **271**, 1339-1347.
21. Meng, J., N. Sakata, S. Takebayashi, T. Asano, T. Futata, R. Nagai, K. Ikeda, S. Horiuchi, T. Myint and N. Taniguchi. 1998. Glycoxidation in aortic collagen from STZ-induced diabetic rats and its relevance to vascular damage. *Atherosclerosis* **136**, 355-365.
22. Mikhailov, V., M. Mikhailova, D. J. Pulkrabek, Z. Dong, M. A. Venkatachalam and P. Saikumar. 2001. Bcl-2 prevents Bax oligomerization in the mitochondrial outer membrane. *J. Biol. Chem.* **276**, 18361-18374.
23. Muradian, K. and D. O. Schachtschabel. 2001. The role of apoptosis in aging and age-related disease: update, Z. *Gerontol. Geriatr.* **34**, 441-446.
24. Naumann, U., J. Wischhusen, S. Weit, J. Rieger, H. Wolburg, U. Massing and M. Weller. 2004. Alkylphosphocholine-induced glioma cell death is BCL-X(L)-sensitive, caspase-independent and characterized by massive cytoplasmic vacuole formation. *Cell Death Differ.* **11**, 1326-1341.
25. Oltvai, Z. N., C. L. Milliman and S. J. Korsmeyer. Bcl-2 heterodimerizes *in vivo* with a conserved homologue, Bax that accelerates programmed cell death. 2003. *Cell* **74**, 609-619.
26. Pollack, B. S., B. K. Park and B. P. Yu. 1996. 4-Hydroxyhexenal is a potent induces of the mitochondrial permeability transition. *J. Biol. Chem.* **271**, 6033-6038.
27. Pollack, J. J., H. Bertrand and B. P. Yu. 1995. Inhibition of adenine nucleotide translocator by lipid peroxidation products. *Free Radic. Biol. Med.* **19**, 583-590.
28. Pollack, M. and C. Leeuwenburgh. 2001. Apoptosis and aging: role of the mitochondria. *J. Gerontol. Biol. Sci. Med. Sci.* **56**, 475-482.
29. Pollack, R., F. Marcheselli, F. Moroni and C. Pieri. 2002. Apoptosis in human aortic endothelial cells induced by hyperglycemic condition involves mitochondrial depolarization and is prevented by N-acetyl-L-cysteine. *Metabolism* **51**, 1384-1388.
30. Pryor, W. A., R. Cueto, X. Jin, W. H. Koppenol, M. Ngu-Schwemlein, G. L. Squadrito, P. L. Uppu and R. M. Uppu. 1995. A practical method for preparing peroxynitrite solutions of low ionic strength and free of hydrogen peroxide. *Free Radic. Biol. Med.* **18,** 75-83.
31. Ruef, J., M. Moser, C. Bode, W. Kubler and M. S. Runge. 2001. 4-Hydroxynonenal induces apoptosis, NF-κB-activation and formation of 8-isoprostane in vascular smooth muscle cells. *Basic Res. Cardiol.* **96**, 143-150.
32. Schonfeld, P. and R. Bohnensack. 1997. Fatty acid-promoted mitochondrial permeability transition by membrane depolarization and binding to the ADP/ATP carrier. *FEBS Lett.* **420**, 167-170.
33. Toyokuni, S., K. Uchida, K. Okamoto, Y. Hattori-Nakakuki,

H. Hiai and E. R. Stadtman. 1994. Formation of 4-hydroxy-2-nonenal-modified proteins in the renal proximal tubules of rats treated with a renal carcinogen, ferric nitrilotriacetate. *Proc. Natl. Acad. Sci.* **91**, 2616-2620.
34. Uchida, K. 2000. Role of reactive aldehyde in cardiovascular diseases. *Free Radic. Biol. Med.* **28**, 1685-1696.
35. Uchida, K. 2003. 4-Hydroxy-2-nonenal: a product and mediator of oxidative stress. *Prog. Lipid Res.* **42,** 318-343.
36. Usatyuk, P. V. and V. Natarajan. 2004. Role of mitogen-activated protein kinases in 4-hydroxy-2-nonenal-induced actin remodeling and barrier function in endothelial cells. *J. Biol. Chem.* **279,** 11789-11797.
37. Wang, D. S., N. Iwata, E. Hama, T. C. Saido and D. W. Dickson. 2003. Oxidized neprilysin in aging and Alzheimer's disease brains. *Biochem. Biophys. Res. Commun.* **310**, 236-241.
38. West, J. D., C. Ji and L. J. Marnett. 2005. Modulation of DNA fragmentation factor 40 nuclease activity by poly (ADP-ribose) polymerase-1. *J. Biol. Chem.* **280**, 15141-15147.
39. Yang, J., X. Liu, K. Bhalla, C. N. Kim, A. M. Ibrado, J. Cai, T. I. Peng, D. P. Jones and X. Wang. 1997. Prevention of apoptosis by Bcl-2: release of cytochrome c from mitochondria blocked. *Science* **275**, 1129-1132.
40. Yu, B. P. and H. Y. Chung. 2001. Oxidative stress and vascular aging, Diabetes Res. *Clin. Pract.* **2**, 73-80.
41. Zamzami, N., P. M. Marchetti, C. Castedo, J. L. Zanin, P. Vayssiere, X. Petit and G. Kroemer. 1995. Reduction in mitochondrial potential constitutes an early irreversible step of programmed lymphocyte death *in vivo. J. Exp. Med.* **181**, 1661-16672.

초록 : 4-Hydroxynonenal의 미토콘드리아 탈분극을 통한 혈관 내피 세포의 세포사 유도기전

강대연[1,3†] · 이지영[1,2†] · 김민선[1] · 김철홍[1,3] · 김형근[1,3] · 이선미[1,3] · 권영미[1,3] · 이재원[1] · 백형석[3] · 유병팔[4]
정해영[1]*
([1]부산대학교 약학대학 약학과, [2]부산대학교 허혈조직재생센터, [3]부산대학교 유전공학연구소, [4]텍사스주립대학 건강과학센터)

4-Hydroxynonenal (4-HNE)는 세포내 레독스의 균형을 깨뜨려 혈관 기능 손상을 일으킨다. 본 연구자들은 HNE의 축적이 야기하는 혈관 기능 손상기전을 더 잘 이해하기 위하여 혈관 내피 세포의 미토콘드리아 세포사 메커니즘을 규명하였다. HNE를 처리한 세포에서는 미토콘드리아 막전위 소실과 그에 따른 cytochrome C의 방출이 유도되었으며, Bax의 증가 및 Bcl-2의 감소가 관찰되었다. ROS 제거제인 NAC와 peroxynitrite 제거제인 페니실라민은 HNE가 유도하는 ROS 생성을 차단하여 cytochrome C 방출과 세포사를 억제하였다. 세포에 HNE와 zVAD-fmk (caspase 저해제)를 같이 처리하면 HNE가 유도하는 세포사를 억제하지 못하는데 이는 HNE에 의한 세포사가 caspase에 비의존적 단계일 가능성을 시사하였다. 위의 결과들은 HNE가 유도하는 혈관 내피 세포의 세포사 매커니즘은 미토콘드리아 막전위의 탈분극에 의해 촉발되며 이는 혈관계 항상성의 악화와 노화에 의해 수반되는 혈관 기능 손상을 유도할 것으로 사료된다.